A NOVEL FEM APPROACH FOR THE ANALYSIS OF TYPE-IV HYDROGEN STORAGE TANK BASED ON THE ENHANCED REFINED ZIGZAG THEORY ECCOMAS CONGRESS 2024

FILIPPO VALORIANI[12], GIUSEPPE CREDO[2] AND MARCO GHERLONE[1]

[1] Department of Mechanical and Aerospace Engineering (DIMEAS)
Politecnico di Torino
10129 Turin, Italy

[2] Department of Virtual Engineering and NVH
Dumarey Automotive Italia S.p.A.
10129 Turin, Italy

Key words: Hydrogen storage, Composite pressure vessel, Filament wound composites, Refined Zigzag theory

Summary. Hydrogen is one of the best energy carriers for renewable energy storage due to its high energy density per unit mass. Type-IV composite pressure vessels are the current cutting-edge solution for compressed hydrogen gas storage and they represent the current state-of-the art for hydrogen fuel-cell vehicles. These multilayered composite vessels are generally produced by filament winding, a technology that allows for good flexibility in design and a very dense deposition of reinforcing fibre relative to the amount of matrix. Critical issues arise in the modelling by finite elements of the dome-shaped tank structure, since in this area both the thickness and the fibre orientation of each layer vary as a function of the radius and the laminate can be globally thick. These properties cause finite-element modelling using 2D First-order Shear Deformation Theory (FSDT) to be inaccurate, on the other hand, a much more accurate discretization with solid 3D elements leads to computationally costly models. The present paper investigates the modelling of multilayered composite pressure vessels by means of shell finite elements based on the enhanced Refined Zigzag Theory (en-RZT). en-RZT, originated from the FSDT, is adopted to provide accurate and computationally affordable predictions of the global responses for thick laminates with high transverse flexibility and heterogeneity. The study highlights the accuracy and robustness of the developed elements with respect to the complexity of the vessel's stacking sequences. The accuracy and computational burden of the proposed approach is assessed by a comparison with shell finite elements present in the commercially available software.

1 INTRODUCTION

Hydrogen can be an important energy vector for medium-long range transportation, including air,[1] sea, and land transport. Among the various storage methods, compressed hydrogen gas stored in composite overwrap pressure vessels (COPV) represents the state-of-the-art for

hydrogen fuel-cell vehicles.[2–4] Type-IV composite pressure vessels are typically manufactured using filament winding,[5] this method allows for a very high fiber content relative to the matrix and provides significant design flexibility also for complex geometries[6] and stacking sequences.[7] However, these features present challenges in the accurate finite element modelling of the structure, particularly when employing conventional modelling techniques.[8,9]

The aim of this article is to compare current numerical validation techniques in order to assess the practicability of introducing a new finite element that enables the study of complex structures without affect to computationally expensive models.

To achieve this, a new solver (ZZen Garden) was developed, which implements a finite element based on recent advancements in the enhanced refined zigzag theory.[10,11]The results show that this new approach can replace, at least for the analyses presented, computationally expensive models that require commercial codes. The paper is organized as follows. In the Materials section, two different approaches to stacking sequence generation are presented, along with the finite element and the formulation it is based on, followed by the test cases considered for the analyses. In the Results section, the outcomes are reported and discussed, with appropriate comparisons with elements from commercial software.

2 MATERIALS

2.1 Modelling approaches and formulation

As we can see in figure 1 the properties of the stacking sequence as: number of plies, thicknesses and orientations, vary along the tank.

When designing a COPV, it is necessary to take into account the variation of stacking sequences as one moves along the axis of revolution of the tank. In the design phase, a stacking sequence is determined for the cylindrical area of the tank, then, it is possible to automatically determine an algorithm that evolves this stacking sequence as a function of radius and provides us with all possible laminations for the dome area. This process can leads to different stacking sequences definition approach.

Considering a generic stacking sequence, table 1, we propose two methods that will return slightly different outcomes. The aim is that the algorithm automatically assigns to certain finite elements a different stacking sequence evolving that of the cylindrical area. Figure 2 for a visual description.
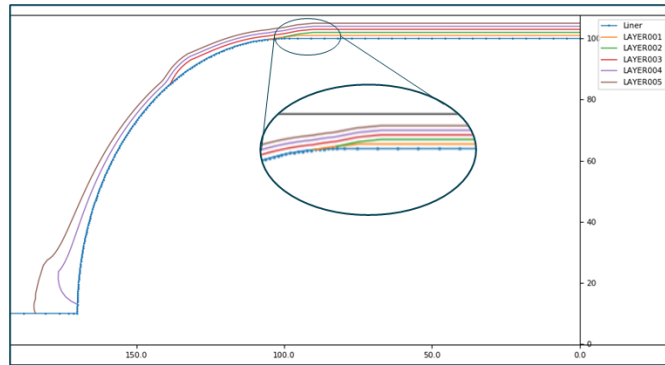

Figure 1: Section of a tank design, focus on cylinder-dome transition region

- WoundSim[12] approach, we will refer to as: not oriented (**NOR**)

  - All layers are oriented at 0°, every layer has a different materials that consider the rotation angle

- PyTank approach, we will refer to as: oriented (**OR**)

  - Every layer has its own orientation angle, every layers got the same materials, as design.

These differences affect the composition of the laminate stiffness matrices. Particularly for the not oriented case, the stiffness components that couple unidirectional and in-plane shear stresses are always zero.

Table 1: Generic stacking sequence

# layers	6
Thickness [mm]	$3/1 \times 5$
Angles [degree]	$0/89/88/60/10/8$
Material	HDPE / CFRP$\times 5$

2.1.1 Enhanced refined zigzag finite element

Considering a generic solid made of multilayered plate, figure 3 (a), and an orthogonal Cartesian coordinate system defined by the vector $\mathbf{X} = \{x_1, x_2, x_3\}$. The vector $\mathbf{x} = \{x_1, x_2\}$ represents the set of in-plane coordinates on the reference plane, here chosen to be the middle plane of the solid, and x_3 being the coordinate normal to the reference plane. The thickness of each layer, as well as of the whole plate, is assumed to be constant, and the material of each layer
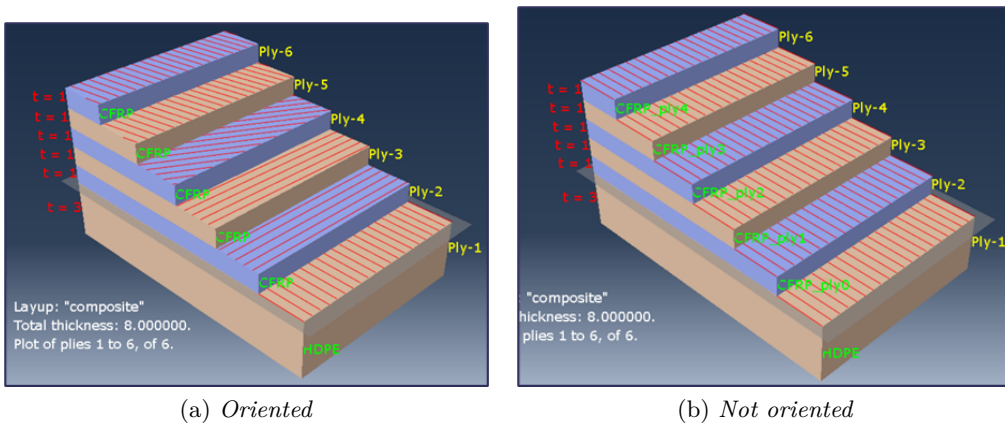

(a) *Oriented*   (b) *Not oriented*

Figure 2: Stacking sequence for PyTank and WoundSim

3

is assumed to be elastic orthotropic with a plane of elastic symmetry parallel to the reference surface and whose principal orthotropy directions are arbitrarily oriented.

According with the kinematic presented by Sorrenti and Di Sciuva,[10,11] the displacement field is

$$
\begin{aligned}
U_1^k &= u_1(\mathbf{x};t) + x_3\theta_1(\mathbf{x};t) + \Phi_{11}^k(x_3)\psi_1(\mathbf{x};t) + \Phi_{12}^k(x_3)\psi_2(\mathbf{x};t) \\
U_2^k &= u_2(\mathbf{x};t) + x_3\theta_2(\mathbf{x};t) + \Phi_{21}^k(x_3)\psi_1(\mathbf{x};t) + \Phi_{22}^k(x_3)\psi_2(\mathbf{x};t) \\
&\qquad\qquad\qquad\qquad\qquad\qquad\qquad U_3^k = w(\mathbf{x};t)
\end{aligned}
\tag{1}
$$

Where u_α and θ_α ($\alpha = 1,2$) are the global uniform displacement, and rotations of the normal, to the reference plane plane. ψ_α are the unknown spatial amplitudes of the $\Phi^k(x_3)$ zigzag functions (assumed continuous piecewise linear vanishing to top and bottom external surfaces). In figure 3 (b), a qualitative representation of the zigzag functions and their effect on the displacement field.

Based on this formulation and on the previous work of Gherlone, Versino and Zarra.[13] A new finite element has been developed. The finite element is a quadrilateral flat shell element named **En-RZT Q4**, main features are:

- Enhanced zigzag function to allow coupling effect in angle-ply laminates

- Interdependent interpolation strategy to avoid shear locking

- Added drilling degree of freedom to work on curved structures

- Stabilization procedure to eliminate spurious mode

- Possibility to define Material Reference System to orient the stacking sequence.

The En-RZT Q4 element has been integrated inside a finite element python code: ZZen Garden. ZZen Garden take in input a file generated by Hypermesh or PyTank (in-house Dumarey code), the input file contains information regarding the mesh, loads and constraints. While the properties of element sets are entered by the user via an excel sheet.
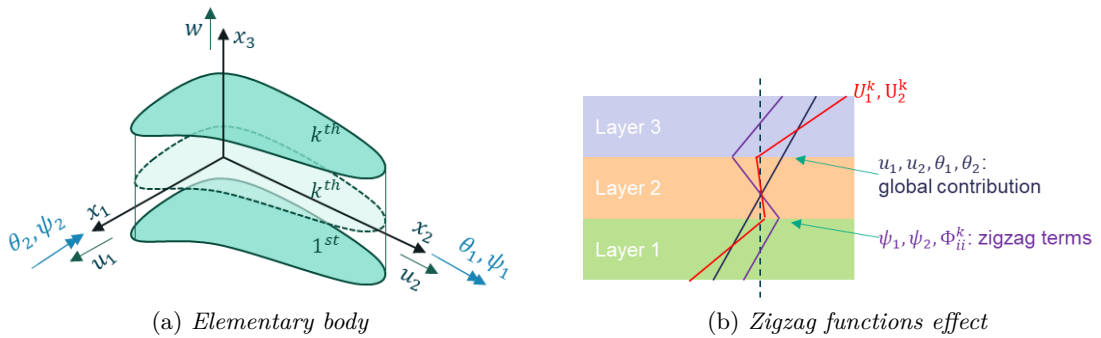

(a) *Elementary body*   (b) *Zigzag functions effect*

Figure 3: Zigzag formulation

2.2 Test cases

We refer to Carbon Fiber Reinforced Polimer material as CFRP. In table **??** we present the materials properties used in the structures.

Table 2: CFRP properties

|	CFRP	Al	Foam
Young's modulus [MPa]	135000/9660/9660	69000	900
Poisson ratio	.25/.25/.41	0.3	0.46
Shear's modulus [MPa]	5860/5860/3460		
Density [tonn/mm^3]	$1.8e^{-9}$	$2.7e^{-9}$	$9.5e^{-10}$

2.3 Cylinder sandwich

Cylinder with sandwich lamination, lower edge clumped and upper edge free. We compare the natural frequencies obtained with the model meshed with en-RZT Q4 elements against other meshes using finite elements from commercial software

In figure 4(a) a layout of the structure with its own stacking sequence in table 4(b). In figure 5 a visualisation of the mesh with en-RZT Q4 elements and that with CHEXA20 elements, from Hypermesh, where the big difference in terms of number of nodes and elements can be highlighted.

2.4 Cantilevered plate

A cantilevered plate clumped on one edge with a uniform distributed load applied on whole surface. Stacking sequence is similar to that which could characterise a tank. Using different mesh we perform a comparison on static and modal analysis as follow

- Natural frequencies and shape function

- Max displacements of the static analysis in the two free extreme vertices, referred to as P1 and P2
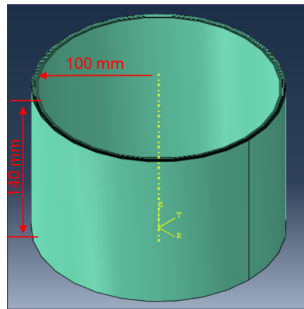
(a) *Cylinder*

Radius/high [mm]	100/140
# layers	3
Thickness [mm]	1.5/2/1.5
Angles [degree]	0/0/0
Material	Al/Foam/Al

(b) *stacking sequence*

Figure 4: Cylinder sandwich

- Stresses through the thickness in point with coordinates $y = 33b/40$ and $x = 7b/40$

In figure 6(a) a layout of the structure with its own stacking sequence in table 6(b). Again shows, in figure 7, the considerable difference between en-RZT Q4 and CHEXA20 meshes. On right image, wee can also see the vertices P1 and P2, and the point for stress extraction

2.5 Tank

Half tank with realistic stacking sequence. On the half tank symmetric boundary condition are applied: u_y, θ_x, θ_z are constrained for the lower cylindrical edge, in upper dome edge we constrain u_x, u_z, θ_y. In the results we show the difference between the oriented and non-oriented lamination approach, using the en-RZT Q4 element compared with the ABAQUS C3D8.

In figure 8(a) the meshed structure. The stacking sequence in table 8(b) is related to the cylinder part of the vessel. Each coloured rings on the dome correspond to a different stacking sequence, generated by evolving the cylinder stacking sequence.

3 RESULTS

CQUAD4 is a 4 node quadrilater flate shell element from optistruct, based on the Reissner-Mindlin formulation. CHEXA8 and CHEXA20 are respectively cubic elements at 8 and 20 nodes, from optistruct too. C3D8R, C3D20 are respectively cubic elements at 8 with reduced integration and 20 nodes not reduced integration, from ABAQUS.

3.1 Cylinder

In table 3 we can quantitatively appreciate the huge difference, in terms of degrees of freedom, between reduced 2D models and more accurate models with 3D elements. When working with 3D elements these numbers are unavoidable as many elements must be inserted along the thickness of each ply. To maintain reasonable aspect ratios (< 5), the size of the elements in the plane is reduced, so the overall number goes up.

Table 4 shows the first 10 natural frequencies. Given the symmetry, the frequencies are coupled. $err\%$ is the average relative error of the first fifteen frequencies respect to CHEXA20, equation 2 with $I = N = 15$
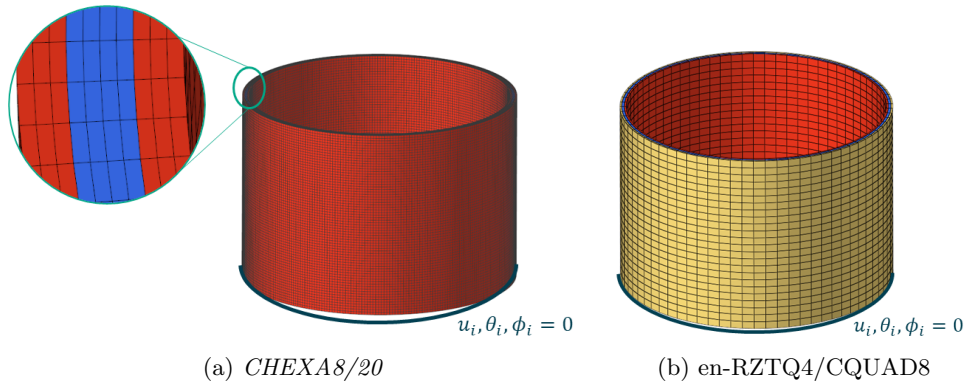

(a) *CHEXA8/20* (b) en-RZTQ4/CQUAD8

Figure 5: Cylinder mesh

(a) *Structure layout*

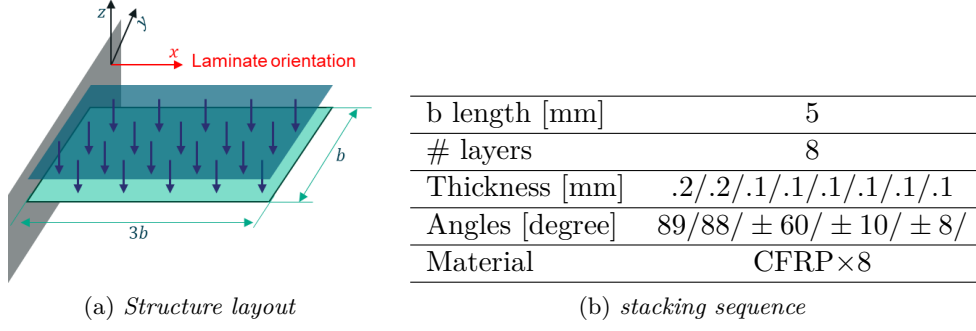| b length [mm]	5
# layers	8
Thickness [mm]	.2/.2/.1/.1/.1/.1/.1/.1
Angles [degree]	89/88/ ± 60/ ± 10/ ± 8/
Material	CFRP×8

(b) *stacking sequence*

Figure 6: Cantilevered plate layout

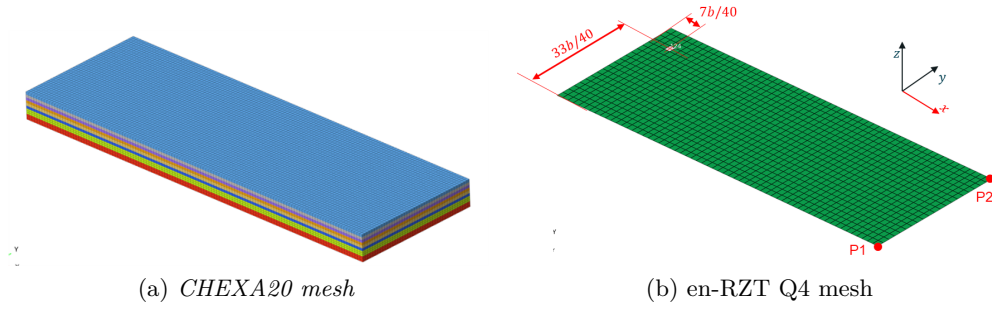$$err\% = \frac{1}{N} \sum_{i=1}^{I} \left(\frac{f_i - f_{i_{CHEXA20}}}{f_{i_{CHEXA20}}} \times 100 \right) \tag{2}$$

(a) *CHEXA20 mesh*

(b) en-RZT Q4 mesh

Figure 7: Cantilevered plate mesh

(a) *Half tank mesh*

Radius/high [mm]	100/220
# layers	8
Thickness [mm]	1/1/.5/.5/.5/.5/.5/.5
Angles [degree]	89/88/ ± 60/ ± 10/ ± 8/
Material	CFRP×8

(b) *stacking sequence*

Figure 8: Half tank

7
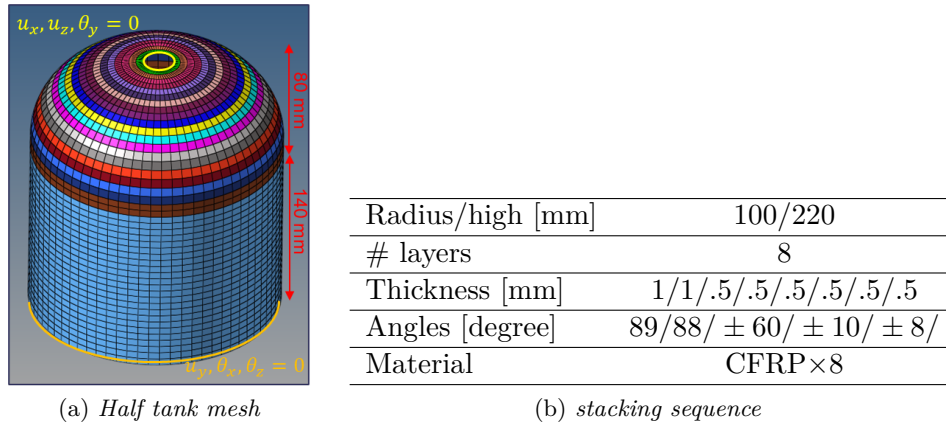
Table 3: Cylinder mesh

	en-RZT Q4	CQUAD4	CHEXA8	CHEXA20
# nodes	1'825	1'825	242'110	943'020
# Dofs	16'425	10'950	726'330	2'829'060

Table 4: Cylinder natural frequencies

Natural freq	en-RZT Q4	CQUAD4	CHEXA8	CHEXA20
f1/2 [Hz]	1447.6	1426.3	1455.7	1455.2
f3/4 [Hz]	1802	1760.7	1814.2	1813.6
f5/6 [Hz]	1818.5	1801.7	1818.8	1818.3
f7/8 [Hz]	2503	2398.8	2494.3	2493.8
f9/10 [Hz]	3106.2	3130.1	3122.6	3122.2
err [%]	0.4	2.5	0.0	/

3.2 Cantilevered

Table 5 shows two characteristic frequencies, relating to a bending mode of vibration and one with bending-torsional coupling, figure 10 for detail. $err\%$ is the average relative error of the first ten frequencies respect to CHEXA20, equation 2 with $I = N = 10$.

Transverse displacement values of the vertices are in table 6. For models with cubic elements, the displacement value considered is obtained by averaging those of the vertex nodes. P1 and P2 $err\%$ are the relative error respect to displacement from CHEXA20 model, equation 3.

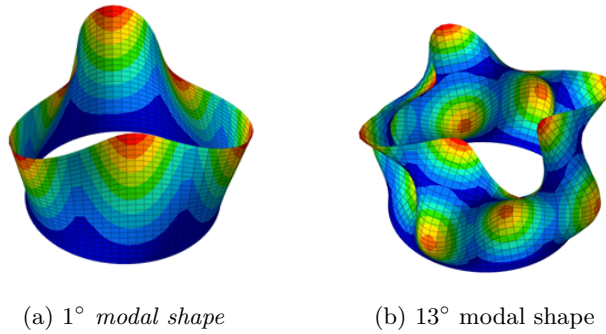$$P1err\% = \frac{w_{P1} - w_{P1_{CHEXA20}}}{w_{P1_{CHEXA20}}} \times 100 \tag{3}$$

(a) 1° *modal shape*　　　　(b) 13° modal shape

Figure 9: Cylinder modal shapes

Table 5: Cantilevered plate natural frequencies

	en-RZT Q4	CQUAD8	CHEXA8	CHEXA20	C3D8R	C3D20
f3 [Hz]	16622.5	16082.5	16519.9	16512.8	16490	16514
f8 [Hz]	73960.1	72244.2	72932	72872.3	72835	72886
err [%]	1.1	3.0	0.1	/	0.1	0.0

Table 6: Cantilevered plate vertices displacements

	en-RZT Q4	CQUAD8	CHEXA8	CHEXA20	C3D8R	C3D20
P1 [mm]	-28.24	-21.9	-28.3	-28.4	-28.5	-28.4
P2 [mm]	-28.97	-22.6	-29.1	-29.1	-29.2	-29.1
P1 err [%]	-0.50	-22.70	-0.10	/	0.30	0.00
P2 err [%]	-0.50	-22.30	-0.20	/	0.30	0.00

3.2.1 Stresses trough thickness

As shown in figure 7(b) for selected element, stresses through the thickness are compared between the various types of finite elements. The exact stresses with which the others are compared are considered to be those from the mesh with second-order solid elements (CHEXA20). We have placed 3 CHEXA20 along the thickness for each ply and stresses are collected in its centroid.

Table 11 contains the root mean square error of the curves, equation 4. Cubic elements from both Hypermesh and ABAQUS return almost identical results. A good reconstruction of stresses is observed, especially for those in the plan, by en-RZT Q4 model. The Mindlin element (CQUAD4) shows major errors and is probably not suitable for applications on multilayer structures with major thicknesses. In the tank models we will use exclusively the en-RZT Q4.

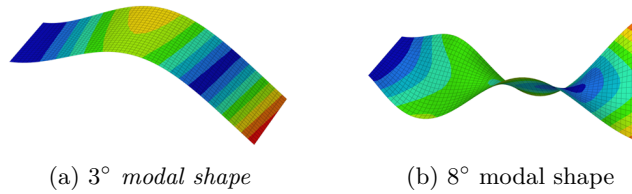$$RMSE\% = 100 \times \sqrt{\frac{1}{N} \sum_{i=1}^{I} \left(\frac{\sigma_i - \sigma_i^m}{\sigma_{MAX}^m} \right)^2} \tag{4}$$

(a) 3° *modal shape*   (b) 8° modal shape

Figure 10: Cantilevered plate modal shapes

Table 7: Cantilevered plate vertices displacements

RMSE [%]	en-RZT Q4	CQUAD8	CHEXA20	C3D20
σ_{11}	1.40	9.50	/	0.90
σ_{22}	12.60	87.60	/	8.50
σ_{12}	3.90	14.10	/	2.10
σ_{13}	80.70	133.70	/	8.40
σ_{23}	32.60	58.70	/	5.50

3.3 Tank

For computational reasons, half tank model uses C3D8 elements with not optimal refinement along the thickness: just one element per ply. In the following results, we will compare a model generated using WoundSim and analyzed in Abaqus with a model generated using PyTank and analyzed with ZZen Garden. The comparison is limited to certain modal shapes and the observation of the effect of the oriented and non-oriented laminate on the static deformation.

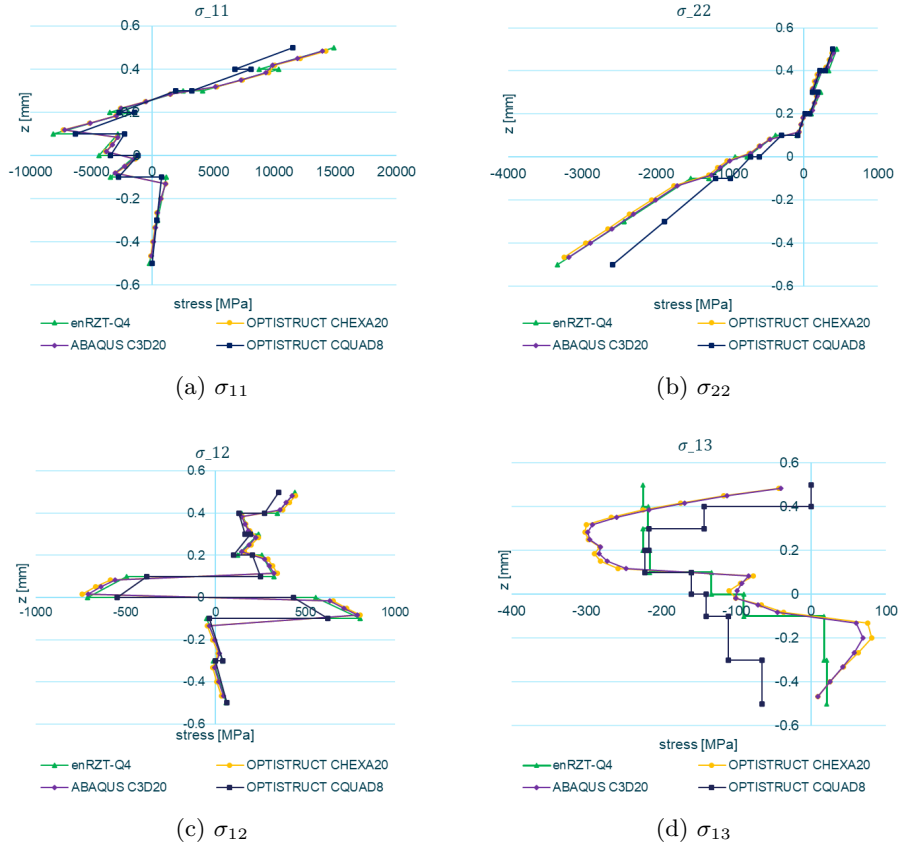In static deformation, the effect of stacking sequence approach is noticeable. Figure 13(a)

(a) σ_{11}

(b) σ_{22}

(c) σ_{12}

(d) σ_{13}

Figure 11: Cantilivered plate stresses

10

shows the displacement in length direction, while figure 13(b) shows the displacement in x-direction. (b) image it can be observed that the expansion of the tank, due to internal pressure, also causes a torsion around its axis, an effect not present in the case of a non-oriented laminate.

4   CONCLUSIONS

The aim of this paper was to investigate the state of the art in composite tank modeling and explore potential improvements through alternative stacking sequence methods and new finite elements. While the analyses conducted by Nebe[7,8] and Berro[9] achieved excellent results, they rely on computationally expensive models that offer limited flexibility for design modifications and optimization, which often require numerous adjustments and quick analyses.

The study highlights how a finite element based on enhanced refined zigzag theory can be a accurate and computationally efficient tool in analysis of COPV. En-RZT Q4 elements can be effectively utilized in the design and optimization of composite structures. Moreover, the study indicates the value of using in-house software for tank model reconstruction, such as PyTank, has proven capable of accurately reconstructing varying stacking sequences along the vessel's length. Combined with ZZen Garden, PyTank provides a reliable framework for composite tank design and validation from the initial layout through to final validation. The research provides an improved understanding of the torsion effects related to different stacking sequences modelling techniques, although further investigation needed.

These results are promising and encourage further development of the methodology, with critical next steps including progressive failure analysis, nonlinear behavior, and more complex stacking sequence algorithms.
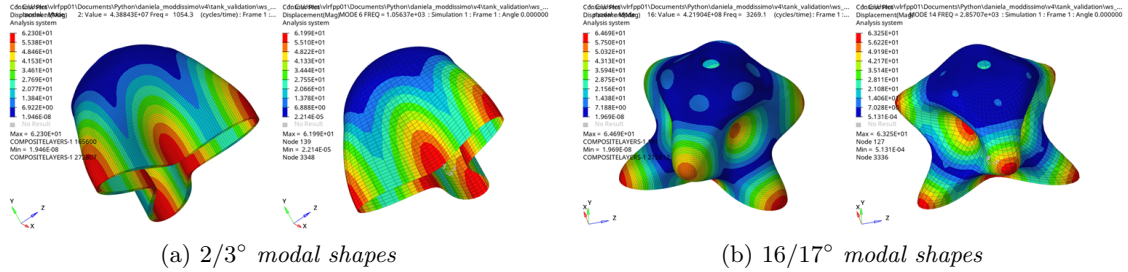

(a) 2/3° *modal shapes*   (b) 16/17° *modal shapes*

Figure 12: Half tank modal shapes. C3D8 NOR - en-RZT Q4 OR

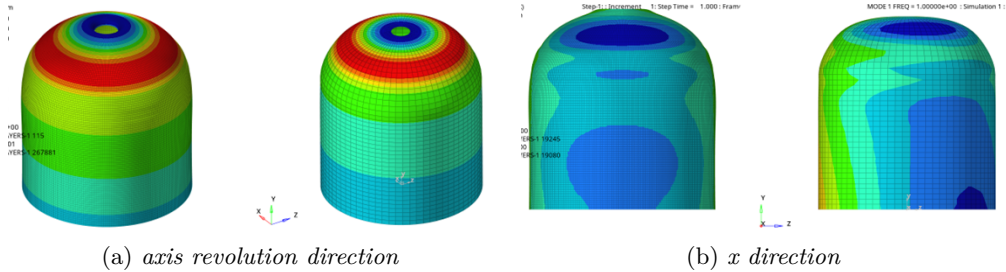(a) *axis revolution direction*   (b) *x direction*

Figure 13: Half tank deformation. C3D8 NOR - en-RZT Q4 OR

11

REFERENCES

[1] Romeo, G., Danzi, F., Cestino, E., Borello, F., 2013. "Design and Optimization of a Composite Vessel for Hydrogen Storage Subject to Internal Pressure and In-Flight Loads for UAVs" International Journal of Aerospace Sciences, DOI: 10.5923/j.aerosp ace.20130203.05

[2] Yamashita, A., Kondo, M., Goto, S., and Ogami, N. 2015. "Development of High-Pressure Hydrogen Storage System for theToyota "Mirai"," SAE Technical Paper 2015-01-1169, doi:10.4271/2015-01-1169.

[3] Yahashi, H., Yamashita, A., Shigemitsu, N., Goto, S. et al. 2021. "Development of High-Pressure Hydrogen Storage System for New FCV," SAE Technical Paper 2021-01-0741, doi:10.4271/2021-01-0741.

[4] Hassan, I.A. ; Ramadan, Haitham S., Saleh, Mohamed A., Hissel, Daniel. 2021. "Hydrogen Storage Technologies for Stationary and Mobile Applications: Review, Analysis and Perspectives." Renewable & sustainable energy reviews 149

[5] Azeem, Mohammad et al. 2022. "Application of Filament Winding Technology in Composite Pressure Vessels and Challenges: A Review." Journal of energy storage 49

[6] Früh, Nikolas, and Jan Knippers. 2021. "Multi-Stage Filament Winding: Integrative Design and Fabrication Method for Fibre-Reinforced Composite Components of Complex Geometries." Composite structures 268

[7] Nebe, M., Johman, A., Braun, C., van Campen, J.M.J.F. 2022. "The Effect of Stacking Sequence and Circumferential Ply Drop Locations on the Mechanical Response of Type IV Composite Pressure Vessels Subjected to Internal Pressure: A Numerical and Experimental Study." Composite structures 294

[8] Nebe, M, Soriano, A., Braun, C., Middendorf, P., Walther, F. 2021. "Analysis on the Mechanical Response of Composite Pressure Vessels during Internal Pressure Loading: FE Modeling and Experimental Correlation." Composites. Part B, Engineering 212

[9] Berro Ramirez, Juan Pedro et al. 2015. "700 Bar Type IV High Pressure Hydrogen Storage Vessel Burst – Simulation and Experimental Validation." International journal of hydrogen energy 40.38

[10] Sorrenti, M., and Di Sciuva, M. 2021. "An Enhancement of the Warping Shear Functions of Refined Zigzag Theory." Journal of applied mechanics 88.8

[11] Sorrenti, M., Di Sciuva, M., and Tessler, A. 2021. "A Robust Four-Node Quadrilateral Element for Laminated Composite and Sandwich Plates Based on Refined Zigzag Theory." Computers & structures 242

[12] S Vertical, WoundSim, accessed: 2024-08-31. `https://www.svertical.com/woundsim`

[13] Gherlone, M., Versino, D., and Zarra, V. 2020. "Multilayered Triangular and Quadrilateral Flat Shell Elements Based on the Refined Zigzag Theory." Composite structures 233